



Slavica Ilijević, University of Novi Sad, slavicailljevic7@gmail.com
Sanja Grekulović, University of Belgrade, sanjag@grf.bg.ac.rs
Miljana Todorović Drakul, University of Belgrade, mtodorovic@grf.bg.ac.rs

VALIDATION OF THE NEQUICK AND IRI MODELS BASED ON DATA FROM IONOSONDES

Abstract

This study compares the NeQuick and IRI ionospheric models using data from ionosondes as reference. Validation based on data obtained by direct measurement using ionosondes helps to refine empirical models and improves their reliability. In this way, it is possible to identify the differences and limitations of the model and contribute to its improvement. As the NeQuick and IRI models provide tools for the study of ionospheric variability and forecasts of the ionospheric TEC coefficient, their versions are constantly being improved and need to be validated accordingly. Therefore, this research is based on the comparison of the TEC coefficient for the validation of two different ionosphere models based on data from three different regions of Europe.

Keywords: TEC, IRI, NeQuick, ionosphere, validation, ionosond

ОЦЕЊИВАЊЕ МОДЕЛА NEQUICK И IRI НА ОСНОВУ ПОДАТАКА ИЗ ЈОНОСОНДИ

Сажетак

Ово истраживање упоређује NeQuick и IRI моделе јоносфере користећи као референтне податке мјерења добијених примјеном јоносонди. Валидација на основу података добијених директним мјерењем путем јоносонди помаже у усавршавању емпиријских модела и побољшава њихову поузданост. На тај начин омогућава се идентификовање разлика и ограничења модела и доприноси његовом побољшању. Како NeQuick и IRI модели пружају алате за проучавање варијабилности јоносфере и прогнозе TEC коефицијента у јоносфери, њихове верзије се стално унапређују и потребно их је сходно томе валидирати. Због тога ово истраживање је базирано на упоређењу TEC коефицијента за валидацију два различита модела јоносфере на основу података са три различита региона Европе.

Кључне ријечи: TEC, IRI, NeQuick, јоносфера, валидација, јоносонда

1. INTRODUCTION

The validation of ionospheric models is crucial for ensuring the accuracy and reliability of predictions used in various applications, such as satellite communication, navigation systems, and space weather monitoring. Among the widely used ionospheric models, NeQuick and IRI (International Reference Ionosphere) stand out for their extensive utilization and application across diverse fields. Comparing model outputs with data from ionosondes provides valuable insights into their performance under different conditions. This validation process helps researchers identify any discrepancies or limitations in the models and refine them accordingly. By analyzing data from ionosondes, researchers can assess the models' ability to predict ionospheric behavior accurately. Improving the accuracy of ionospheric models is crucial for enhancing various applications, including satellite communication and GPS navigation. Furthermore, validated models contribute to better space weather forecasting, which is vital for safeguarding sensitive technological systems. The validation of NeQuick and IRI models based on data from ionosondes aids in advancing our understanding of ionospheric physics. It also facilitates the development of more reliable tools for studying and monitoring ionospheric variability. The practical implications of this research extend to a wide range of industries and sectors that rely on accurate ionospheric models for operational purposes. Ultimately, the validation of NeQuick and IRI models represents a significant step forward in improving the reliability and effectiveness of ionospheric modeling for various applications.

The ionosphere, a region in Earth's atmosphere, exhibits remarkable dynamism, with electron density undergoing significant spatial and temporal variations. These fluctuations are influenced by various factors, including altitude, geomagnetic location, time of observation, seasonal variations, solar cycle, and geomagnetic field activity. Given the complexity of ionospheric dynamics, accurate modeling of ionospheric parameters is crucial for a wide range of applications, including communication, navigation, and space weather forecasting.

In this context, the goal of the research is to assess the accuracy of two prominent ionospheric models, namely the International Reference Ionosphere (IRI) and NeQuick, by comparing their predictions with ionosonde measurements. Ionosondes provide direct measurements of electron density profiles in the ionosphere, serving as ground-truth data for validating ionospheric models.

By conducting this comparison, the study aims to evaluate the performance of the IRI and NeQuick models across different geographical locations, geomagnetic conditions, and temporal scales. Understanding the strengths and limitations of these models is essential for improving ionospheric modeling capabilities and enhancing the reliability of ionospheric parameter predictions. Ultimately, the research seeks to contribute to advancements in space weather forecasting and the development of more accurate models for ionospheric characterization.

2. IONOSPHERE AND GNSS SIGNALS

The ionosphere, a dynamic region of Earth's atmosphere, plays a crucial role in the propagation of GNSS signals. Its composition of charged particles interacts with radio waves emitted by GNSS satellites, causing delays and distortions in signal transmission. Understanding ionospheric behavior is essential for accurately interpreting GNSS measurements and mitigating navigation errors caused by ionospheric disturbances.^[10]

The layers at altitudes ranging from approximately 60 km to 2000 km contain a relatively large number of electrically charged atoms and molecules, constituting the ionospheric region. Depending on the level of ionization, the ionosphere is divided (Figure 1.) into four primary layers: D (60-90 km), E (90-140 km), F1 (140-210 km), and F2 (above 210 km).

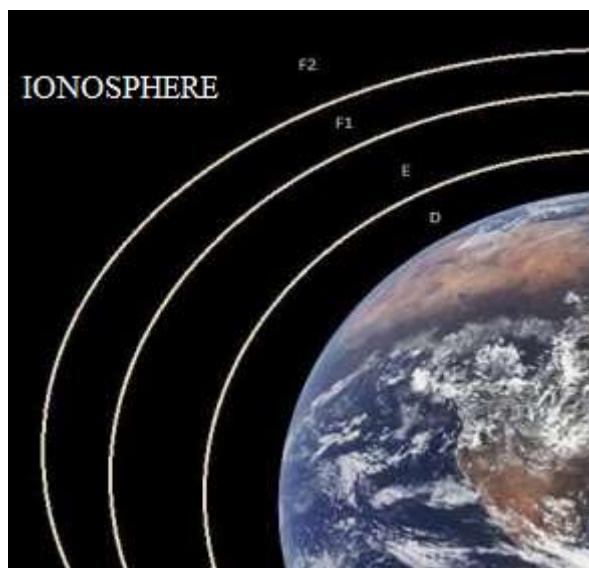


Figure 1. Dividing of ionosphere

2.2. ATMOSPHERE

The Earth's atmosphere is composed of various gases, with oxygen making up only 21%, alongside nitrogen, argon, and trace amounts of other gases like carbon dioxide and methane. It's divided into four main layers: troposphere, stratosphere, mesosphere, and thermosphere, each with distinct characteristics in temperature and composition. The troposphere, closest to the Earth's surface, contains the majority of the atmosphere's mass and is where weather phenomena occur. The stratosphere, with its increasing temperature, contains the ozone layer that shields the Earth from harmful ultraviolet radiation. The mesosphere is where meteors burn up upon entry. The thermosphere, with its high temperatures, is interesting because phenomena like the Northern and Southern Polar Lights and houses satellites and the International Space Station. Beyond these layers, the exosphere merges with space. Additionally, the atmosphere is crucial for signal propagation in navigation systems like GNSS, with the troposphere and ionosphere being particularly relevant. Understanding the dynamics of the atmosphere, especially the ionosphere, is essential for accurate satellite positioning.^{[10][11]}

2.3. COMPOSITION OF THE IONOSPHERE

The ionosphere is formed due to three main factors: solar characteristics, Earth's magnetic field, and Earth's atmosphere. Solar radiation, including X-rays, ultraviolet light, visible light, and radio waves, interacts with Earth's atmosphere, particularly at the top, where the solar constant is approximately 1370 W per square meter. Earth's magnetic field influences the flow of ionized plasma from the Sun, shaping the ionosphere around the planet. Electric currents in Earth's core create the magnetosphere, extending into space. The atmosphere, spanning from sea level to about 1000 km altitude, is divided into several layers based on temperature, ionization, and signal propagation capabilities. The ionosphere, a dynamic region within Earth's atmosphere, undergoes spatial and temporal changes in electron density, influenced by factors such as altitude, geomagnetic location, solar cycle, and season. It consists of four main layers: D, E, F1, and F2. Geomagnetic latitude significantly affects electron density formation in the ionosphere, with notable differences between equatorial, mid-latitude, and high-latitude regions.

In recent years, ionospheric research has been focused on determining the most accurate Total Electron Content (TEC) coefficient using the IRI and NeQuick models, along with ionosonde data from the DIDB (Digital Ionogram Database) website. Studies such as those by Smith et al. (2021)^[1] and Wang et al. (2022)^[2] have explored methodologies for improving TEC predictions and assessing model reliability, while works such as those by Jones and Brown (2023)^[3] and Chen et al. (2023)^[4] have analyzed model performance during geomagnetic storms and seasonal variations. Additionally, research has included the integration of data from various sources, such as combining ionosonde data and models to enhance real-time predictions, as demonstrated by Garcia and Patel (2024)^[5]. Model performance evaluations under different geographic and geomagnetic conditions, as well as in urban areas with high levels of electromagnetic interference, have been highlighted in studies

such as those by Kim et al. (2024)^[6] and Zhang et al. (2024)^[7]. These works collectively represent a step towards better understanding ionospheric processes and improving the accuracy of TEC predictions. Furthermore, studies like those by Li and Wang (2024)^[8] and Sato et al. (2024)^[9] have compared model performance with raw GNSS data to better understand the interactions between the ionosphere and GNSS signals, providing deeper insights into ionospheric dynamics in real terrain conditions.

2.4. THE INFLUENCE OF THE IONOSPHERE ON GNSS SIGNALS

The ionosphere, influenced by various factors including solar electromagnetic radiation and Earth's magnetic field, significantly impacts radio communication, navigation, aviation, and GNSS. Total Electron Content (TEC) is a crucial parameter affecting ionospheric characteristics. GPS measurements are prone to errors categorized into satellite-related, signal propagation environment, receiver, and other errors. Dual-frequency GPS receivers effectively mitigate ionospheric delays, while single-frequency receivers can be accurate with local ionospheric models but less suitable for long baselines. Ionospheric TEC models can correct ionospheric effects for accurate data processing under specific conditions.^{[10][12][13]}

3. IONOSPHERE MODELS

The ionosphere, a complex atmospheric layer, is modeled using various approaches, including empirical, numerical, analytical, and physical models. Empirical models utilize measurements and statistical analyses, while numerical maps represent ionospheric parameters globally or regionally. Analytical models rely on mathematical functions fitted to numerical data, and physical models are based on the physical equations governing electron and ion movement in the ionosphere. Each type of model offers unique insights into ionospheric behavior and is utilized for different applications, such as GNSS signal correction and understanding ionospheric processes.

3.1. NEQUICK MODEL

NeQuick is a sophisticated model designed to predict electron density in the ionosphere. Integrated into the Galileo navigation system, it plays a crucial role in calculating ionospheric effects affecting signal accuracy, particularly for users relying on a single frequency. Based on the ITU-R NeQuick model, it utilizes empirical data to predict monthly average electron density values, considering various parameters like sunspot numbers, solar flux, geographical coordinates, altitude, and universal time. To operate in real-time for Galileo users with single-frequency points, NeQuick uses the "Effective Ionization Level" parameter, derived from coefficients transmitted by Galileo satellites. Its versatility lies in providing corrections for ionospheric delay in vertical and slant directions by integrating projected electron density along the satellite-receiver line. Additionally, NeQuick adjusts for daily changes in solar activity and local geomagnetic conditions, enhancing correction accuracy and navigation precision. The Galileo single-frequency application algorithm involves calculating coefficients and integrating electron density values to obtain Slant Total Electron Content (STEC), which is then converted to meters for compatibility.

$$I_f = \frac{4.3 \cdot 10^{16}}{f^2 [\text{Hz}]} \text{TEC} \quad (1)$$

This formula represents the ionospheric correction factor (I_f) as a function of Total Electron Content (TEC) and frequency (f). The constant (4.3×10^{16}) is multiplied by TEC and divided by the square of the frequency (f) in Hertz. This formula quantifies the impact of TEC on the ionospheric correction factor, which is essential for accurate signal propagation in radio communication and satellite navigation systems. These ionospheric corrections obtained from the NeQuick model are universally applicable to any GNSS signal, provided the correct frequency is set. With NeQuick 2, the latest iteration developed in collaboration between ICTP in Trieste, Italy, and the University of Graz, Austria, significant advancements have been made, promising improved performance and accuracy in predicting ionospheric effects for enhanced satellite navigation systems like Galileo.^{[10][15]}

3.2. IRI MODEL

The International Reference Ionosphere (IRI) project, developed under Committee on Space Research (COSPAR) and International Union of Radio Science (URSI), aims to create a

comprehensive model of Earth's ionosphere for global prediction and analysis. Initiated in the 1960s, the IRI model has undergone multiple versions, with significant advancements introduced since its inception, including updates in 1978, 2001, 2007, and 2012. Its structure comprises global models tailored to distinct ionospheric regions (D, E, F1, and F2 layers), factoring in variables such as solar activity, geomagnetic conditions, and geographic location. These models provide detailed electron density profiles crucial for forecasting ionospheric conditions across various Earth locations. Modified CCIR models are utilized to compute peak electron densities in regions like F2, F1, and E, with different coefficient sets for continental and oceanic areas.^{[10][16]} The height of the F2 peak, is calculated from $M(3000)F_2$ using the empirical formula (Bilitza and Eyfrig, 1979):

$$h_{F_2} = \frac{1490}{M(3000)F_2 + DM} - 176 \quad (2)$$

where the correction factor is calculated as:

$$DM = \frac{f_1 \cdot f_2}{\left(\frac{f_0 F_2}{f_0 E - f_3}\right) + f_4} \quad (3)$$

with solar activity function:

$$f_1 = 0.00232R_{12} + 0.222 \quad (4)$$

$$f_2 = \frac{1 - R_{12}}{150 \exp \exp} \quad (5)$$

$$f_3 = 1.2 - 0.0116 \exp \exp \left(\frac{R_{12}}{41.84} \right) \quad (6)$$

$$f_4 = \frac{0.096(R_{12} - 25)}{150} \quad (7)$$

where R_{12} is the mean annual solar number of sunspots, and Ψ is the magnetic dip latitude.

IRI employs both geodetic and magnetic coordinate systems to capture ionospheric characteristics at different altitudes, enabling accurate modeling of electron density distributions and peak heights. While effective in mid-to-high latitudes, the IRI model faces challenges in equatorial regions during heightened solar activity, necessitating enhancements for better accuracy. To address this, historical satellite data from missions like Alouette and ISIS are integrated to refine parameters and improve predictive capabilities, particularly in regions prone to significant ionospheric variability.

DIDB doesn't use a specific formula itself; rather, it collects, stores, and provides access to ionospheric data obtained from ground-based ionosonde measurements. Ionograms contain information about the time it takes for radio waves to travel through the ionosphere and reflect back to the ground, allowing researchers to derive electron density profiles. Various algorithms and processing techniques may be applied by researchers to analyze ionogram data and derive electron density profiles, but DIDB itself is primarily a repository for this data rather than a tool for data analysis.

3.3. DIGITAL IONOGRAM DATABASE -DIDB

The DIDB is a centralized platform storing digitized ionograms, which represent plasma density profiles in the ionosphere obtained from ground-based ionosonde measurements. This database facilitates access to ionospheric data for researchers worldwide, enabling analysis and utilization for various scientific studies and applications. DIDB contains a vast collection of ionogram records gathered from ionosonde stations globally, offering valuable insights into electron density distribution at different altitudes and times. Researchers can search the database based on specific criteria such as time, location, frequency, and ionosonde type, retrieving ionogram images, raw data, and associated metadata for further analysis. Access to digitized ionogram data via DIDB promotes collaboration and knowledge sharing among the scientific community, contributing to advancements in ionospheric research and space science.

4. COMPARISON MODELS

This section of the paper involves comparing the two models mentioned earlier (NeQuick and IRI) using the TEC coefficient. The results and differences for both models will be compared for each of the following stations in cities (Figure 2.):

- Tromso - Norway (TRO100NOR)

- Prague - Czech Republic (WTZA00DEU)
- Nicosia - Cyprus (ISTA00TUR)



Figure 2. Map with positions of the cities whose TEC coefficients were compared in these research paper.

Three stations in Europe were selected for comparison, situated at different geographical latitudes: northern, central Europe, and the southern part. The stations were chosen in this manner due to the variation in ionospheric influence based on geographical latitude. The objective is to observe the alignment of these models depending on the different station positions. Since the data-collecting stations were not operational simultaneously, it was necessary to find stations that operated in the same year, day, and time. The NeQuick model displayed the years of operation for each station, while for the IRI model, only the application version available on the official website was allowed to be chosen. Here, IRI 2016 was used, knowing that data was available until 2016. The model for the year 2020 did not yield any results, so the previous 2016 model was chosen for consistency. After comparison and research, the three mentioned cities Tromsø, Prague, and Nicosia were selected for the corresponding year.

In addition to comparing these two models, they were also compared with DIDB data directly taken from ionosondes. These data served as reference data for the validation of both models.

4.2. NEQUICK, IRI AND DIDB WEB ENVIRONMENT

The computation of ionospheric coefficients for modeling was conducted using the web applications NeQuick (Figure 3) and IRI (Figure 4), accessible at the following URLs: <https://t-ict4d.ictp.it/nequick2/gps-tec-calibration-online> and <https://kauai.cmc.gsfc.nasa.gov/instantrun/iri/>, respectively. Accurate station names were obtained from the Ionosondes – DIDB website (<https://giro.uml.edu/didbase/scaled.php>), facilitating precise identification of each station.

These web applications are open to all users, and their utilization is permitted to everyone. While the NeQuick model link provides access solely to the TEC coefficient, additional coefficients can be obtained within a specified time interval at the following link: <https://t-ict4d.ictp.it/nequick2/nequick-2-web-model>.

The NeQuick web application features straightforward input and output data procedures. Users are required to input the station name, date, and specified time interval for data retrieval. The output provides TEC coefficients for the designated hourly time interval.

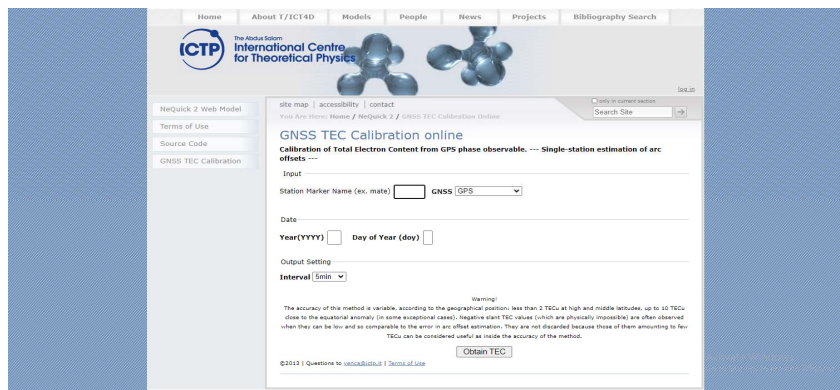


Figure 3. NeQuick web environment

The results were obtained for the specified time interval, with data collected every hour. For each of the three stations and for the onset of each season, TEC coefficients and histograms were generated for every hour.



Figure 4. IRI web environment

The IRI web application presents a slightly more intricate interface compared to the previous NeQuick application. Here, users must input the type of time, date, time, coordinate type (including all three coordinates), as well as data related to terrain profile, as the results are obtained by altitude. To obtain data for every hour, it was necessary to continuously adjust the time. While the IRI application averages data over time, it still presents variations by altitude. The need for constant time adjustment was the primary challenge with this web application. Unlike the NeQuick application, all parameters in the IRI model are derived for a single station. In addition to the TEC parameter, various other parameters such as electron density, electron temperature, ion temperature, ion composition (O⁺, H⁺, He⁺, N⁺, NO⁺, O²⁺, ion clusters), equatorial vertical ion drift, F1 probability, F spread probability, auroral boundaries, and the effects of ionospheric storms on F and E density thresholds were also obtained.

On the EPS website, stations can be searched by name or via a map display, where circles mark the cities where stations are located. Clicking on a station name opens a window containing information about its exact position in various reference systems, as well as various other details related to all European stations. The data available on the EPS, along with the use of the aforementioned models, are accessible to all users, downloadable in any format, and free to use. Calculation time intervals occur every hour during the first day of each season.

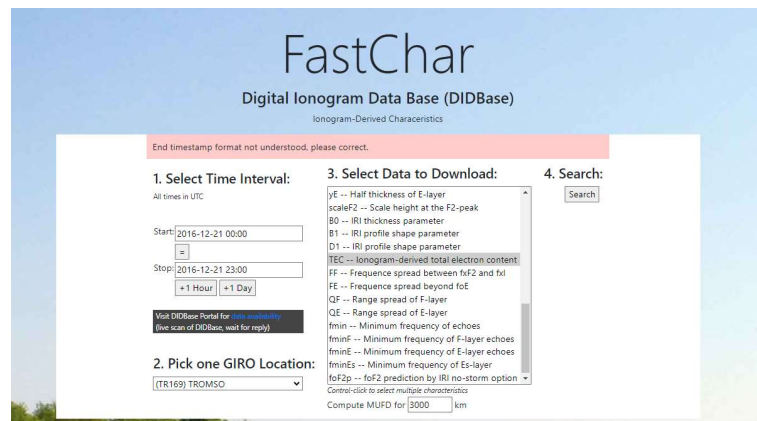


Figure 5. DIDB web environment

The DIDB web interface (Figure 5) offers a user-friendly experience. Users need to specify the required time interval, locate the station, select the data type, and click "Search." Upon searching for the specified time interval, operational stations during that period are displayed. However, the opening of a new window with data does not guarantee data availability. The time interval search provides the TEC coefficient for a specific time, which may not be available for every hour or minute due to sporadic data collection. In cases where exact hourly values are unavailable, they were either approximated to the nearest full hour or marked as missing within a reasonable interval, denoted by "?".

The Digital Ionogram Database (DIDB) does not employ a specific formula itself; instead, it gathers, stores, and offers access to ionospheric data obtained from ground-based ionosonde measurements. Ionograms provide insights into the time taken for radio waves to traverse the ionosphere and reflect back to the ground, aiding in the derivation of electron density profiles. Researchers utilize various algorithms and processing techniques to analyze ionogram data and derive electron density profiles. DIDB primarily serves as a repository for this data rather than a tool for data analysis.

4.3. CALCULATIONS OF NEQUICK AND IRI MODEL TEC COEFFICIENTS FOR THE BEGINNING OF EACH SEASON

Calculations for the first day of each season are chosen because temperature changes are more significant compared to other days throughout the year. In the next subsection, NeQuick and IRI model TEC coefficients will be presented for all four initial days of the seasons during 2016. This year is selected because all the data for all three cities were available during that year.

In the following subsections, the TEC coefficients obtained through calculations in the NeQuick and IRI models will be compared with the data from ionosondes for this city.

The selection of the three cities, Tromso, Prague, and Nicosia, situated at diverse geodetic latitudes, representing the northern, central, and southern regions of Europe respectively, facilitates a comprehensive comparison, enabling the observation of distinct TEC variations corresponding to latitude differences.

Tromso is a city in northern Norway. The name of this station is TRO100NOR and coordinates are:

$$\varphi = 69.60$$

$$\lambda = 18.20$$

$$h = 138.00 \text{ m}$$

In the central part of Europe, the Prague is station in Czech Republic - GOPE00CZE. The geodetic coordinates of this city are:

$$\varphi = 50.00$$

$$\lambda = 14.60$$

$$h = 592.60 \text{ m}$$

In the southern part of Europe are not find a station, the only one was on the Asian peninsula, Nicosia is the city in Cyprus (NICO00CYP) with coordinates:

$$\varphi = 35.03$$

$$\lambda = 33.16$$

$$h = 190.10 \text{ m}$$

which contains data for the first days of the seasons in 2016.

4.3.1. SPRING (20.03.2016)

Based on Figures 6, 7, and 8, depicting the graphs for the first day of Spring for each of the cities where TEC was measured, it can be concluded that the coefficient values in the IRI model were closer to the reference model DIDB compared to NeQuick. Above Prague around 14.00, the TEC coefficient in the NeQuick model was better than in the IRI model, but after that hour, the IRI model performed better.

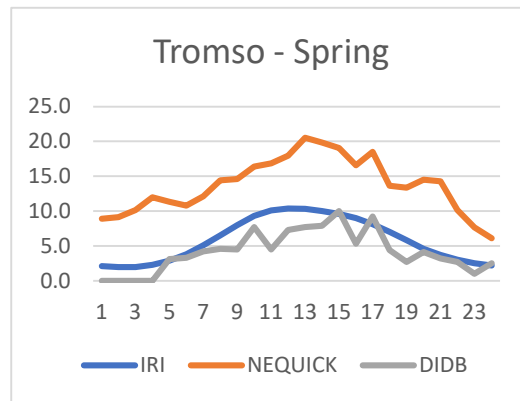


Figure 6. TEC coefficient above Tromso hourly on 1st day of Spring 2016

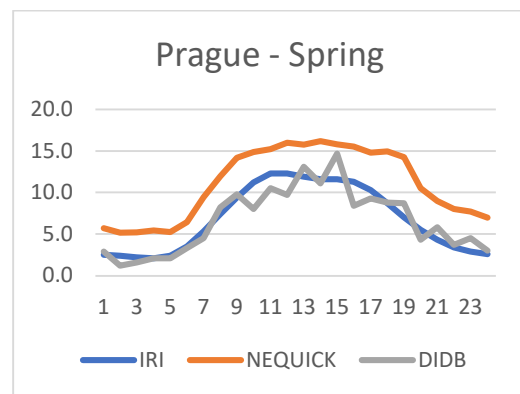


Figure 7. TEC coefficient above Prague hourly on 1st day of Spring 2016

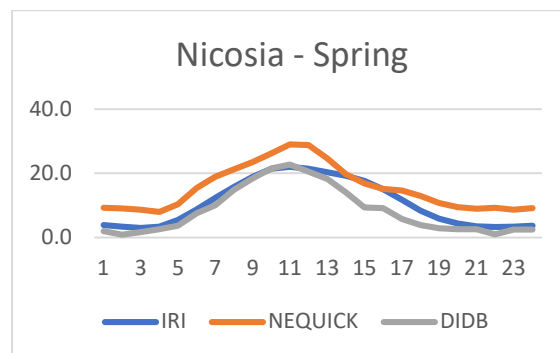


Figure 8. TEC coefficient above Nicosia hourly on 1st day of Spring 2016

Comparing the IRI and NeQuick models:

- The maximum value in the city of Tromso was observed in the NeQuick model at 12.00, with TEC amounting to 20.5. Above Prague in the NeQuick model at 1.00 o'clock is TEC value 10.0 and above Nicosia at 13.00 hours, also in the NeQuick model value of TEC is 16.2.
- The minimum TEC value above Tromso was observed in the IRI model at 2.0, occurring at 1.00 and 2.00 during the night. TEC value above Prague was 1.1 at 19.00 in the IRI model, and above Nicosia at 3.00 over the night was 2.1 on the IRI model, too.

4.3.2. SUMMER (21.06.2016)

During the first day of summer (Figures 9, 10, and 11), the IRI model is closer to the DIDB reference model compared to the NeQuick model - this can be observed in the graphs presented immediately below.

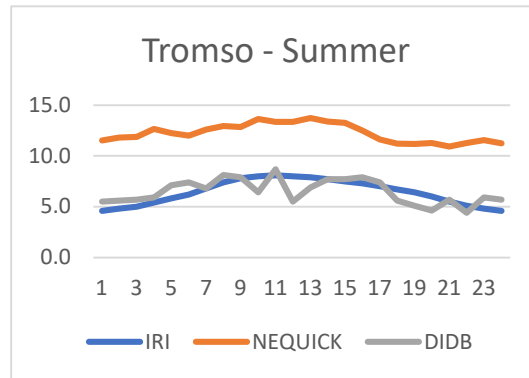


Figure 9. TEC coefficient above Tromso hourly on 1st day of Summer 2016

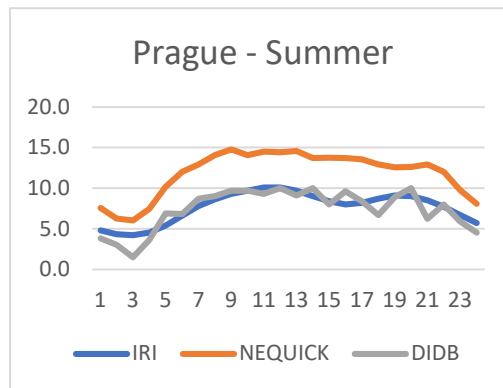


Figure 10. TEC coefficient above Prague hourly on 1st day of Summer 2016

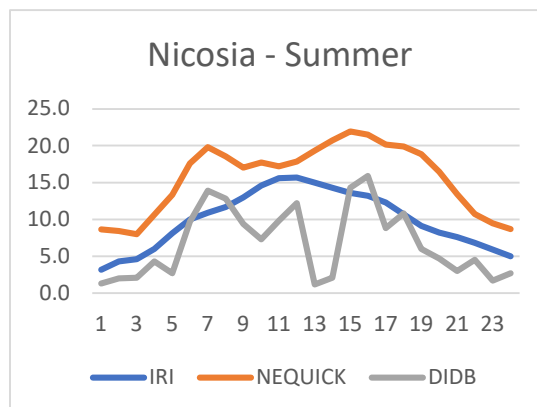


Figure 11. TEC coefficient above Nicosia hourly on 1st day of Spring 2016

The maximum TEC coefficient above the cities was as follows:

- For Tromso, the value was 13.7 in the NeQuick model precisely at noon – 12.00 PM.
- For Prague, the value was 10.0 also in the NeQuick model at 14.8 at 8.00 in the morning.
- For Nicosia, the value was 22.0 (NeQuick) at 14.00.

The minimum TEC coefficient above the cities was as follows:

- For Tromso, the value was 4.6 in the IRI model precisely at midnight – 12.00 AM.
- For Prague, the value was 4.2 also in the IRI model at 2.00 AM.
- For Nicosia, the value was 3.2 in the IRI model, at the same time as Tromso, at 00.00.

4.3.3. AUTUMN (22.09.2016)

On Autumn, the approximation of TEC coefficients by the IRI and NeQuick models above Tromso, Prague, and Nicosia, compared to the values from DIDB - ionosondes, was better with the IRI model. Over the course of 14 hours above Prague, the TEC coefficient in the NeQuick model closely approached the DIDB value, yet once again, the IRI model proved to be a better approximation – Similar situation in Spring above the Prague in the same time. (Figure 12, 13 and 14)

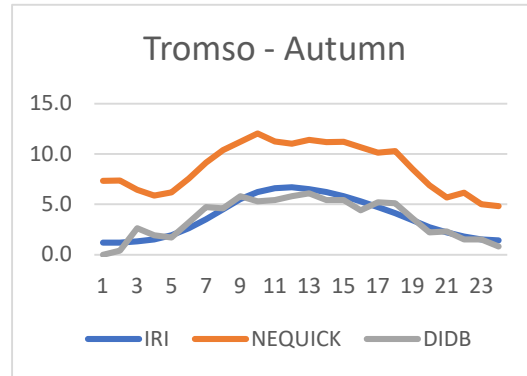


Figure 12. TEC coefficient above Tromso hourly on 1st day of Autumn 2016

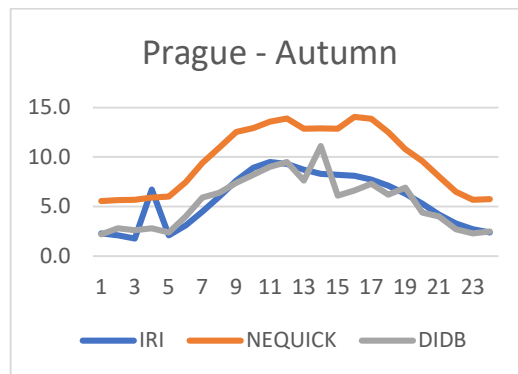


Figure 13. TEC coefficient above Prague hourly on 1st day of Autumn 2016

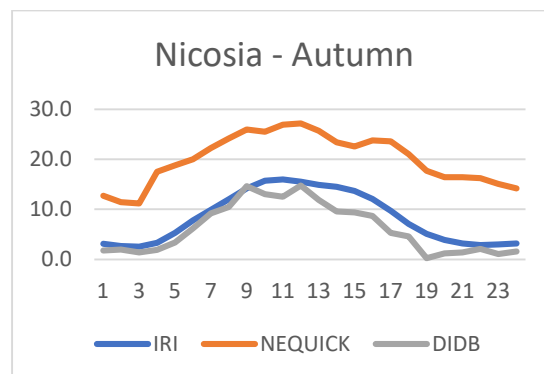


Figure 14. TEC coefficient above Nicosia hourly on 1st day of Autumn 2016

Comparison of the IRI and NeQuick models reveals the highest TEC values above:

- Tromso, with a value of 12.0 at 9.00 a.m. in the NeQuick model
- Prague, reaching 14.1 at 3.00 p.m. in the NeQuick model
- Nicosia, registering 27.2 around 11.00 AM

The lowest TEC values from this comparison above:

- Tromso, recording 1.2 at midnight and 1.00 AM in the IRI model
- Prague, showing 1.8 in the IRI model during the night at 2.00 AM
- Nicosia, indicating 2.6 - in the IRI model also at 2.00 AM

4.3.4. WINTER (21.12.2016)

In winter, as with the other seasons, the IRI model performed better compared to the NeQuick model.

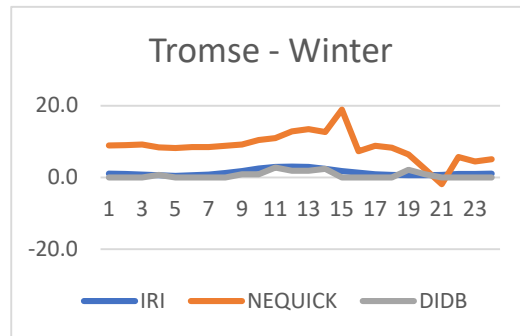


Figure 15. TEC coefficient above Tromso hourly on 1st day of Winter 2016

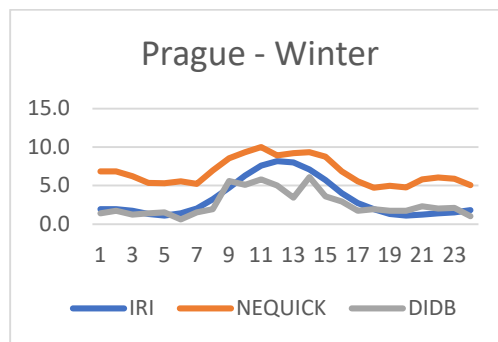


Figure 16. TEC coefficient above Prague hourly on 1st day of Winter 2016

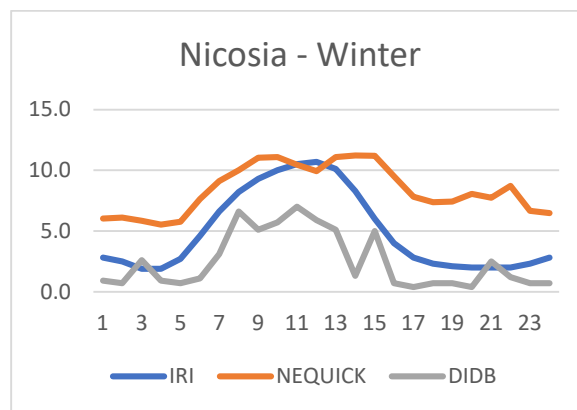


Figure 17. TEC coefficient above Nicosia hourly on 1st day of Winter 2016

On the first day of winter, the maximum value above (Figure 15, 16 and 17):

- Tromso was 13.5 in the NeQuick model at noon, 12.00.
- Prague was in the NeQuick model, specifically 10.0 at 10.00 o'clock.
- Nicosia was around 11.2 at 13.00 and 14.00 o'clock in the NeQuick model.

The minimum values were above:

- Tromso, where the TEC value was 0.55 at 4.00 in the morning according to the IRI model.
- Prague had a TEC coefficient value of 1.1, also at 4.00 in the morning.
- Nicosia had a TEC value of 1.9 at 2.00 and 3.00 in the morning according to the IRI model.

4.3.5. STANDARD DEVIATION IN ALL SEASONS

Table 1 shows the standard deviation between the NeQuick model and the IRI model, between NeQuick and DIDB, and between IRI and DIDB. This table contains data above the city of Tromso in Norway.

Table 1. The table of standard deviation for each first day of the season, above the city of Tromso, comparing both models with each other and both with DIDB data.

Season	MODEL	σ	Max σ	Min σ	Max σ	Min σ
Spring	IRI -NQ	8.78	9.66	2.30	13.06	0.70
	IRI - DIDB	2.30				
	NQ - DIDB	9.66				
Summer	IRI -NQ	5.86	5.86	1.01		
	IRI - DIDB	1.01				
	NQ - DIDB	5.85				
Autumn	IRI -NQ	4.30	5.14	0.70	Winter NQ-IDB	Autumn IRI-DIDB
	IRI - DIDB	1.27				
	NQ - DIDB	4.53				
Winter	IRI -NQ	13.06	13.06	0.95		
	IRI - DIDB	0.95				
	NQ - DIDB	8.60				

From the first table for the city of Tromso in Norway, we can see that the maximum deviation from the reference model was with the NeQuick model, both in the spring, with a standard deviation value of 9,66 and a difference of referent value was 12.8 at 12.00. The minimum standard deviation was in winter with the IRI model, amounting to 0.95, with a difference value of 0.3 at 23.00.

Table 2 shows the standard deviation between the NeQuick model and the IRI model, between NeQuick and DIDB, and between IRI and DIDB. This table contains data above the city of Prague in Czech Republic.

Table 2. The table of standard deviation for each first day of the season, above the city of Prague, comparing both models with each other and both with DIDB data.

Season	MODEL	σ	Max σ	Min σ	Max σ	Min σ
Spring	IRI -NQ	4.30	4.61	1.50	4.61	1.15
	IRI - DIDB	1.50				
	NQ - DIDB	4.61				
Summer	IRI -NQ	4.33	4.56	1.15		
	IRI - DIDB	1.15				
	NQ - DIDB	4.56				
Autumn	IRI -NQ	4.30	4.53	1.27	Spring NQ - DIDB	Summer IRI - DIDB
	IRI - DIDB	1.27				
	NQ - DIDB	4.53				
Winter	IRI -NQ	3.62	4.20	1.46		
	IRI - DIDB	1.46				
	NQ - DIDB	4.20				

In the second table for Prague in the Czech Republic, we see that the maximum deviation from the reference model was either with the NeQuick model in spring, with a standard deviation value of 4.61, and a deviation value of 7.31 at 15.00. The minimum standard deviation is with the IRI model, amounting to 1.15, with a deviation value of 0.2 at 18.00 during first day of summer.

Table 3 shows the standard deviation between the NeQuick model and the IRI model, between NeQuick and DIDB, and between IRI and DIDB. This table contains data above the city of Nicosia in Cyprus.

Table 3. The table of standard deviation for each first day of the season, above the city of Nicosia, comparing both models with each other and both with DIDB data.

Season	MODEL	σ	Max σ	Min σ	Max σ	Min σ
Spring	IRI -NQ	5.11	7.09	3.11	13.96	0.16
	IRI - DIDB	3.11				
	NQ - DIDB	7.09				
Summer	IRI -NQ	6.15	9.55	5.00		
	IRI - DIDB	5.00				
	NQ - DIDB	9.55				
Autumn	IRI -NQ	0.16	13.96	0.16	Autumn NQ - DIDB	Autumn IRI - DIDB
	IRI - DIDB	2.612				
	NQ - DIDB	13.959				
Winter	IRI -NQ	3.968	6.13	3.01		
	IRI - DIDB	3.010				
	NQ - DIDB	6.129				

The largest deviation occurred on the first day of autumn between NeQuick and DIDB, amounting to 13.96, with a deviation value of 1.3 at 16.00. The smallest deviation, also in autumn as in other cases, was between the IRI and DIDB models, with a value of 1.61, and the difference was 0.16 at 8.00 in the morning.

Analyzing the results obtained from the IRI and NeQuick models compared to DIDB as the reference model is complex. Initially, the NeQuick model provided data at half-second intervals, but later, the website was updated, and the selected interval was obtained. Initially, the data were for all satellites and were not averaged, but after the update, an averaged TEC coefficient was obtained, which later facilitated work. IRI was calculated based on the profile, and a change in the TEC coefficient at a certain altitude was observed.

From the tables above, it can be seen that the maximum and minimum values are calculated at approximately the same time during the day, but these values differ. This occurs due to parameters that are either included or not included in the model, as models arrive at TEC coefficients in different ways.

From all the graphs, it can be observed that the TEC coefficient curves obtained by the IRI model are smoother than those obtained by the NeQuick model, which have sharper transitions. Generally, the highest TEC parameter values are obtained for all days for the Nicosia area, and the lowest for the Norwegian area. This is expected because the ionospheric impact is more significant at higher latitudes, the Earth's geomagnetic field is tilted more vertically, resulting in a greater number of ion particles in the ionosphere.

Additionally, it should be noted that the data from the IRI model were taken at a higher node, 1000 m, but it was noticed that changing the maximum height affects the TEC coefficient. Since in this case, the maximum height of 1000 m was taken, the IRI model was closer. It is assumed that by increasing the height profile in IRI, the difference from DIDB data would increase, and NeQuick would perform better. It should also be added that there were no available data for every moment/hour in the DIDB reference model, so that time was not included in the overall calculation, but only with the data that were available.

5. CONCLUSION

Based on the analysis of ionospheric research in recent years, significant progress has been made in understanding and assessing TEC using various models such as IRI and NeQuick, along with integrating ionosonde data from the DIDB website. These models have been extensively studied in the context of different geographic and geomagnetic conditions, as well as in urban areas with high levels of electromagnetic interference. Studies have also focused on improving the accuracy of TEC predictions, particularly during geomagnetic storms and seasonal variations. Additionally, research has highlighted the importance of integrating data from various sources, such as ionosondes and GNSS, to enhance real-time predictions. These work represent a step towards a deeper understanding of ionospheric processes and increasing the accuracy of TEC predictions, which is crucial for various applications in telecommunications, navigation, and space exploration.

5.1. OBSERVATION AND FUTURE RESEARCH

We need to find the reason why significant changes occur in TEC coefficients at 80 km in the IRI model during certain time periods. We should investigate why specifically at 80 km and what disrupts the calculations there.

Both models follow the trend of increasing TEC during daytime hours and decreasing during nighttime, providing good estimates during different seasons. Regarding simplicity and speed of use, the NeQuick model has an advantage because its input and output data are simpler. The IRI model is more complex in terms of the multitude of input coefficients that need adjustment and output information that is not relevant for these purposes, requiring additional time investment.

In any case, in future research, these data should be validated with TEC data obtained from the same stations using original GNSS observations or ionosonde data. This way, we could assess the level of accuracy of these two models and determine, based on a reference model, which of these two models more accurately approximates TEC coefficients.

LITERATURE

- [1] Komjathy, "Global ionospheric total electron content mapping using the global positioning system," 1997. Accessed: Dec. 13, 2023.
- [2] A. Silva, A. Moraes, J. Sousasantos, M. Maximo, B. Vani, and C. Faria, "Using Deep Learning to Map Ionospheric Total Electron Content over Brazil," *Remote Sensing*, vol. 15, no. 2, p. 412, Jan. 2023.
- [3] E. Lake and A. Seyoum, "Performance Evaluation of IRI-Plas 2017 model with Ionosonde Data Measurements of Ionospheric Parameters," *Research Square*, Jan. 17, 2022.
- [4] Chalachew Kindie Mengist, K. Seo, Yong Ha Kim, S. Eswaraiah, N. Ssessanga, and Y. Kwak, "3-D Regional Imaging of Ionosphere Over Africa Through Assimilating Satellite and Ground-Based Data," *Journal of Geophysical Research: Space Physics*, vol. 128, no. 2, Feb. 2023.
- [5] L. Kun et al., "Research on Real Time Reconstruction Technology of Regional Ionospheric Model with GNSS Data Integrated," *Journal of spatial science*, vol. 68, no. 4, pp. 579–591, Oct. 2022.
- [6] D. Mei, X. Ren, X. Le, H. Liu, and X. Zhang, "Ionospheric Tomography: A Compressed Sensing Technique Based on Dictionary Learning," *IEEE transactions on geoscience and remote sensing*, vol. 61, pp. 1–10, Jan. 2023.
- [7] H. Haralambous, K. S. Paul, A. K. Singh, and T. Gulyaeva, "Investigation of the Topside Ionosphere over Cyprus and Russia Using Swarm Data," *Remote Sensing*, vol. 15, no. 5, p. 1344, Jan. 2023.
- [8] B. Maletkii, E. Astafyeva, S. A. Sanchez, E.A. Kherani, and E.R. de Paula, "The 6 February 2023 Türkiye Earthquake Sequence as Detected in the Ionosphere," *Journal of Geophysical Research: Space Physics*, vol. 128, no. 9, Sep. 2023.
- [9] T. O. Osanyin et al., "Performance of a locally adapted NeQuick-2 model during high solar activity over the Brazilian equatorial and low-latitude region," *Advances in Space Research*, vol. 72, no. 12, pp. 5520–5538, Dec. 2023.
- [10] M. Todorović-Drakul, "Моделовање јоносфере за потребе одређивања утицаја на ГПС сигнале у мрежном РТК окружењу," PhD, Faculty of Civil Engineering University of Belgrade, 2016, Accessed: May 23, 2024.
- [11] The Earth's Atmosphere. Berlin, Heidelberg: Springer Berlin Heidelberg, 2008.
- [12] K. G. Budden, *Radio Waves in the Ionosphere*. 2009. Accessed: May 23, 2024.
- [13] M. C. Kelley, *The Earth's Ionosphere: Plasma Physics and Electrodynamics*. Academic Press, 2009. Accessed: May 23, 2024.
- [14] D. Bilitza, "IRI the International Standard for the Ionosphere," *Advances in Radio Science*, vol. 16, pp. 1–11, Sep. 2018.
- [15] A. Pignalberi, M. Pezzopane, D. R. Themens, H. Haralambous, B. Nava, and P. Coisson, "On the Analytical Description of the Topside Ionosphere by NeQuick: Modeling the Scale Height Through COSMIC/FORMOSAT-3 Selected Data," *IEEE Journal of Selected Topics in Applied Earth Observations and Remote Sensing*, vol. 13, pp. 1867–1878, 2020.
- [16] J. G. Sivavaraprasad, and D. Venkata Ratnam, "Performance analysis of IRI-2016 model TEC predictions over Northern and Southern Hemispheric IGS stations during descending phase of solar cycle 24," *Acta Geophysica*, vol. 69, no. 4, pp. 1509–1527, Jun. 2021.